6-1-2007

Energy dispersion relations for holes inn silicon quantum wells and quantum wires

Vladimir Mitin

Nizami Vagidov

Mathieu Luisier

Gerhard Klimeck
Purdue University - Main Campus, gekco@purdue.edu

J Comput Electron (2007) 6:227–230
DOI 10.1007/s10825-006-0103-9

Energy dispersion relations for holes in silicon quantum wells and quantum wires

Vladimir Mitin · Nizami Vagidov · Mathieu Luisier · Gerhard Klimeck

Published online: 9 December 2006

Abstract We calculate the energy dispersion relations in Si quantum wells (QW), $E(\mathbf{k}_{2D})$, and quantum wires (QWR), $E(\mathbf{k}_{1D})$, focusing on the regions with negative effective mass (NEM) in the valence band. The existence of such NEM regions is a necessary condition for the current oscillations in ballistic quasineutral plasma in semiconductor structures. The frequency range of such oscillations can be extended to the terahertz region by scaling down the length of structures. Our analysis shows that silicon is a promising material for prospective NEM-based terahertz wave generators. We also found that comparing to Si QWRs, Si QWs are preferable structures for NEM-based generation in the terahertz range.

Keywords Energy dispersion relations · Tight-binding model · Negative effective mass · Quantum well · Quantum wire

V. Mitin (✉) · N. Vagidov
University at Buffalo, SUNY, 332D Bonner Hall, Buffalo, NY 14260, USA
e-mail: vmitin@buffalo.edu

N. Vagidov
e-mail: nizami@eng.buffalo.edu

M. Luisier
Integrated Systems Laboratory, ETH Zurich, 8092 Zurich, Switzerland
e-mail: mluisier@iis.ee.ethz.ch

G. Klimeck
Network for Computational Nanotechnology, Purdue University, West Lafayette, IN 47907, USA
e-mail: gekco@purdue.edu

1 Introduction

Energy dispersion curves with negative-effective-mass (NEM) regions can be found in bulk semiconductors, quantum wells, quantum wires, as well as in artificially band-engineered structures such as heterostructure obtained by the cleaved edge overgrowth technique (see [1] and references therein). The existence of such NEM regions may lead to current instabilities in ballistic diodes and transistors [2]. For submicrometer base lengths of these devices the frequency of current oscillations falls into the terahertz range. Tight-binding simulations of the energy band structure is an effective tool for identification and engineering of structures with well-pronounced NEM regions in energy dispersions.

In this paper we report the results of band structure calculations of Si quantum wells (QW) and quantum wires (QWR). We calculated the energy dispersion relations, $E(\mathbf{k}_{2D})$ and $E(\mathbf{k}_{1D})$, for different orientations of two-dimensional wavevector, $\mathbf{k}_{2D}$, in QWs and one-dimensional wavevector, $\mathbf{k}_{1D}$, in QWRs. We used an empirical $sp^3d^5s^*$ tight-binding model which takes into account 10 atomic orbitals: s- and excited s^*-orbitals, three p-, and five d-orbitals. The inclusion in the model of higher energy d-orbitals and spin-orbital coupling has dramatically improved the precision of the calculated electron and hole energy dispersion relations. In our calculations we used tight-binding parameters of Si from Ref. [3]. All other details of the exploited model can be found in Ref. [4].

The simplest model of energy dispersion relations with NEM regions is based on anti-crossing of two bands with light and heavy carriers. It can be described by the following equation:

$$E(k) = \frac{1}{2}\left[\varepsilon_1(k) + \varepsilon_2(k) - \sqrt{[\varepsilon_1(k) - \varepsilon_2(k)]^2 + 4\delta^2}\right] \quad (1)$$

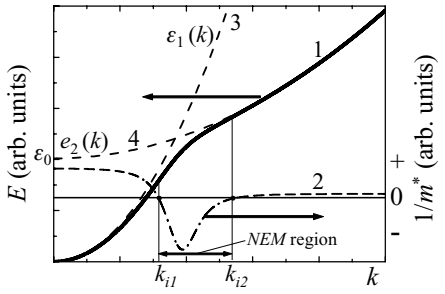

Fig. 1 The graph of $E(k)$ defined by Eq. (1) is shown by solid line 1, inverse effective mass, $1/m^*$, for $E(k)$ is shown by dash-dotted line 2, and two parabolic energy dispersion relations, $\varepsilon_1(k)$ and $\varepsilon_2(k)$, are shown by dashed lines 3 and 4. The region of negative effective mass is located between two inflection points, k_{i1} and k_{i2}

where $\varepsilon_1(k) = \hbar^2k^2/2m$, $\varepsilon_2(k) = \hbar^2k^2/2M + \varepsilon_0$, and $\delta \ll \varepsilon_0$ (see Fig. 1) [5]. Quasineutral semiconductor plasma with current carriers having dispersion $E(k)$ of Eq. (1), may have self-organized oscillatory regimes only at certain ratio of two effective masses, m and M, - light and heavy effective masses, respectively. This ratio must satisfy the following inequality [5]:

$$M/m > 2. \tag{2}$$

Large ratios of M/m are preferable for NEM-based current oscillations to be established.

While this model ignores many important details, it is widely used for qualitative estimates in nonlinear carrier transport. For this reason, in the next sections we will fit our data to the above model.

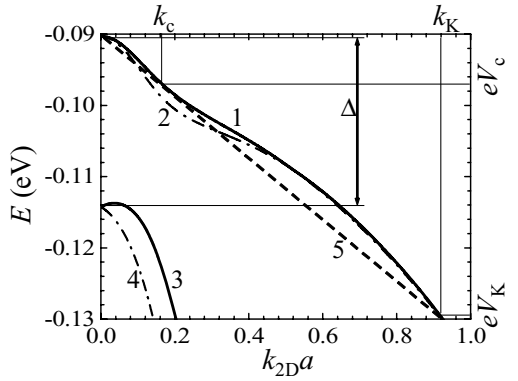

Fig. 2 Dispersion relations $E(\mathbf{k}_{2D})$ for holes in a Si QW for $\mathbf{k}_{2D} \parallel [110]$. The thickness of QW is 2.72 nm. Δ is the energy gap between the lowest and next subband, k_c is a tangency point around which the NEM region is located; k_c and k_K define the beginning and the end of the interval where instability takes place, and a is the Si lattice constant equal to 5.43 Å. Solid lines (1, 3) and dash-dotted lines (2, 4) relate to two energy dispersion relations with opposite spins. Tangent to curve 1 is shown by dashed line 5

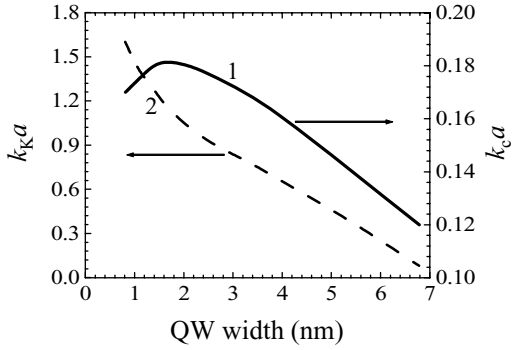

Fig. 3 Dependences of critical values of k_c and k_K on QW width are shown by solid line 1 and dashed line 2, respectively; $k_{2D} \parallel [110]$

2 Energy dispersion relations in Si quantum wells

First, we will present results for Si QWs grown on (100) wafers. Analysis of the peculiarities of the energy dispersion relations associated with the NEM is our main interest here.

We calculated energy dispersion relations $E(\mathbf{k}_{2D})$ for holes in Si QWs with thicknesses from 0.8 nm to 7 nm for $\mathbf{k}_{2D} \parallel [110]$ and $\mathbf{k}_{2D} \parallel [100]$. As an example, $E(\mathbf{k}_{2D})$ of QW with thickness 2.72 nm and $\mathbf{k}_{2D} \parallel [110]$ is shown in Fig. 2. Figure 2 demonstrates well-defined NEM regions, suitable for occurrence of NEM-based current instability, and wide energy interval (eV_c, eV_K) or interval of applied voltage (V_c, V_K), where the stationary current in ballistic semiconductor devices with NEM carriers is unstable. The range of this interval is defined by k_c and k_K, where k_c is the tangency point and k_K is the intersection of tangent and $E(\mathbf{k}_{2D})$, as shown in Fig. 2. Calculated dependences of these two parameters on the well thickness are shown in Fig. 3. The increase of k_c by 50% and increase of k_K by almost factor of 5 with the decrease of thickness of QW leads to a substantial increase of energy interval where the NEM instability exists.

Although, the obtained energy dispersion relations are not described by Eq. (1), qualitatively we can introduce two effective masses, m and M, that characterize calculated $E(\mathbf{k}_{2D})$. As we can see from Fig. 4 the inequality (2) for Si QW with $\mathbf{k}_{2D} \parallel [110]$ is fully satisfied for widths ranging from 0.8 to 7 nm. Another important characteristic of the energy dispersion relations is the energy distance between the lowest and the next subband, Δ. For QWs with thicknesses less than 3 nm this value is about 25 meV. As we can see from Figs. 3 and 4 there is a good control of k_c, k_K, Δ, and M/m over a wide range of QW thicknesses.

In Si QWs with $\mathbf{k}_{2D} \parallel [100]$ the energy dispersion relations do not satisfy the inequality (2) for any QW thicknesses and the NEM regions are weakly pronounced.

In addition, the carried out calculations showed that the Kramers degeneracy [6] of holes at $\mathbf{k}_{2D} \parallel [110]$ is lifted for $\mathbf{k}_{2D} \neq 0$ and there are two different branches of dispersion

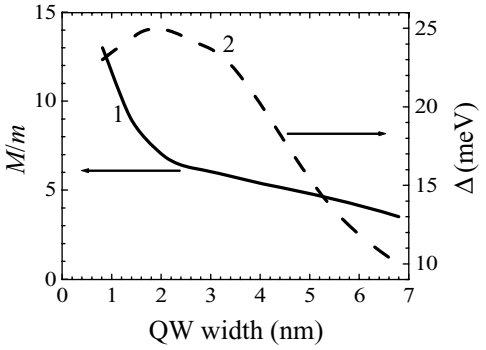

Fig. 4 Dependences of M/m ratio and energy gap Δ on Si QW width for $E(\mathbf{k}_{2D})$ with $\mathbf{k}_{2D} \parallel [110]$ are shown by solid line 1 and dashed line 2, respectively. Dependence on M/m was calculated for the valence band's lowest energy subband

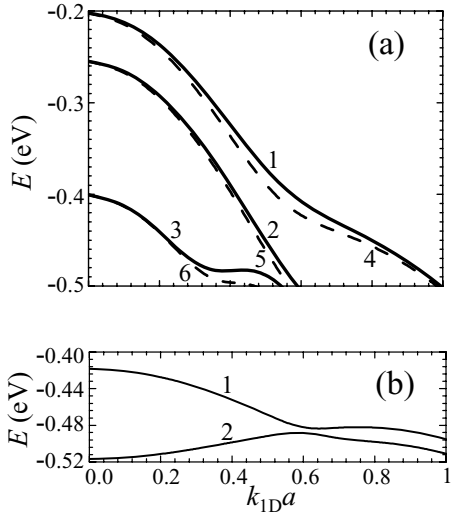

Fig. 5 Dispersion relations $E(\mathbf{k}_{1D})$ for holes in a Si QWR: (a) with cross-section 1.63 × 1.72 nm^2 (in directions [001] and [−110], respectively) and with $\mathbf{k}_{1D} \parallel [110]$; (b) with cross-section 1.63 nm^2 (in directions [001] and [010]) and with $\mathbf{k}_{1D} \parallel [100]$. Solid (1, 2, 3) and dashed (4, 5, 6) lines correspond to holes with opposite spins

relations corresponding to two different spin states as it is seen in Fig. 2 [7]. In contrast to that, for the hole states with wavevector $\mathbf{k}_{2D} \parallel [100]$ the subbands stay spin degenerate for any value of $\mathbf{k}_{2D}$.

3 Energy dispersion relations in Si quantum wires

The calculated Si QWR energy dispersion relations, $E(\mathbf{k}_{1D})$, for $\mathbf{k}_{1D} \parallel [110]$ demonstrate well enough pronounced NEM regions, whereas dispersion curves for $\mathbf{k}_{1D} \parallel [100]$ are almost flat (see Figs. 5(a) and (b)).

The model shows that as in the case of Si QWs, the inequality (2) for energy dispersion relations in QWRs for $\mathbf{k}_{1D} \parallel [100]$ is never satisfied.

Analysis of dependences of inverse effective mass, $1/m^*$, versus $\mathbf{k}_{1D}$ shows that only for QWRs with small cross-

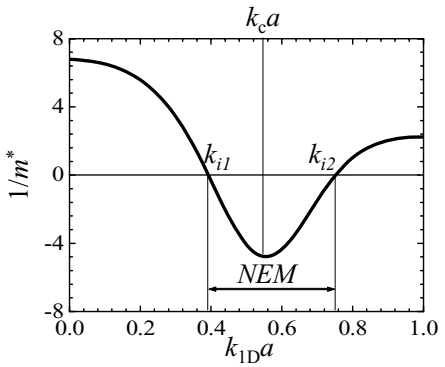

Fig. 6 Dependence of inverse effective mass, $1/m^*$, on $k_{1D}a$ for holes of the lowest energy state in a Si QWR with the cross-section 1.63 × 1.73 nm^2 (in directions [001] and [−110], respectively) and with $\mathbf{k}_{1D} \parallel [110]$. The NEM region is located between two inflection points, k_{i1} and k_{i2}; the ratio $M/m \approx 3$

sections the inequality (2) may be satisfied. An example shown in Fig. 6 for QWR with cross-section 1.63 × 1.73 nm^2 (in directions [001] and [−110], respectively) has the ratio $M/m \approx 3$. If we compare the energy dispersion relations of QWs and QWRs we observe that the energy interval of NEM-induced instability is shifted to higher energies (or higher values of k) in the case of QWRs. The shift of NEM region to higher energies makes it more difficult to maintain ballistic regime of the device.

As in the case of QWs, the spin degeneracy of states for $\mathbf{k}_{1D} \neq 0$ in QWRs with $\mathbf{k}_{1D} \parallel [110]$ is lifted whereas in the case of $\mathbf{k}_{1D} \parallel [100]$ the spin degeneracy is conserved as it is shown in Figs. 5(a) and (b).

4 Conclusion

We calculated energy dispersion relations in Si QWs, $E(\mathbf{k}_{2D})$, and QWRs, $E(\mathbf{k}_{1D})$. The results were obtained for different directions of two-dimensional wavevector, $\mathbf{k}_{2D}$, and one-dimensional wavevector, $\mathbf{k}_{1D}$. The analysis of the obtained dependences shows that the occurrence of NEM-based oscillations are most likely to be found in Si samples in [110] crystallographic direction. Dispersion curves in [100] direction for both QWs and QWRs are flat and their NEM regions do not satisfy the necessary condition for instability occurrence. Another interesting detail is that the energy bands are spin degenerate in [100] direction but the spin degeneracy is lifted in [110] direction for both QWs and QWRs.

The ratio of the effective masses after and before the NEM region, M/m, behaves differently in QWs and QWRs. For QWs in [110] direction this ratio for wide range of well thicknesses is significantly greater than in QWRs. The energy interval of NEM region in QWRs is shifted to higher energies (or higher momenta). This may be an obstacle for maintaining of ballistic oscillatory regime of a device. In

addition, the energy interval of NEM region is smaller in the case of QWRs in comparison to QWs. The fourth parameter that characterizes NEM oscillatory regime, Δ, is the distance between the lowest and the next subbands. The larger is this parameter, the better are the conditions to achieve larger amplitudes of oscillations. And this is the only parameter that is superior in QWRs in comparison with the case of QWs.

In summary, we demonstrate that Si QWs are promising candidates for NEM-based terahertz generation. The data obtained in the framework of empirical tight-binding model can be fitted by the two-band anti-crossing model with the ratio, M/m, changing in the range from 3 to 13 (see Fig. 4). Large values of M/m result in effective current oscillations in wide energy intervals. Using the anti-crossing model, one can estimate the frequencies of generation band [2]. For QW structures with the base lengths 0.1–0.3 μm we obtain the estimates of generation band of 0.5–2 THz.

Acknowledgment This research was supported by Petroleum Research Fund Grant No. 41317-AC10, NSF Grant No. EEC-0228390, and the Indiana 21st Century Fund.

References

1. Gribnikov, Z.S., et al.: Quantum real-space transfer in a heterostucture overgrown on the cleaved edge of a superlattice. J. Appl. Phys. **93**(1), 330 (2003)
2. Gribnikov, Z.S., et al.: Negative-effective-mass ballistic field-effect transistor: Theory and modeling. J. Appl. Phys. **87**(10), 7466 (2000)
3. Boykin, T.B., et al.: Valence band effective-mass expressions in the $sp^3d^5s^*$ empirical tight-binding model applied to a Si and Ge parametrization. Phys. Rev. B **69**(11), 115201 (2004)
4. Rahman, A., et al.: Atomistic approach for nanoscale devices at the scaling limit and beyond – valley splitting in Si. Jpn. J. Appl. Phys. **44**(4B), 2187 (2005)
5. Gribnikov, Z.S., et al.: Terahertz ballistic current oscillations for carriers with negative effective mass. J. Appl. Phys. **80**(10), 5799 (1996)
6. Schmid, U., et al.: Relativistic band structure of Si, Ge, and GeSi: Inversion-asymmetry effects. Phys. Rev. B **41**(9), 5919 (1990)
7. The $sp^3d^5s^*$ model includes spin and spin-orbital coupling explicitly. These simulations do not include any external magnetic field that would provide spin selection. The splitting of the states is purely due to symmetry breaking and the two split states are a mixture of up and down spins